Synthesis and Characterization of Ferroelectric BismuthTitanate ($Bi_4Ti_3O_{12}$)

A dissertation submitted in partial fulfillment of the requirement

for the award of the degree of

Master of Science
in
Physics

Submitted by
Balram
Roll No.-301104006

Under the esteemed guidance of
Dr. Dwijendra P. Singh
(Assistant Professor)

School of Physics and Materials Science
Thapar University
Patiala (Punjab) -147 004

July 2013.

Dedicated

to my

Parents

&

everything

for me

Certificate

This is to certify that the Dissertation entitled ***'Synthesis and Characterization of Ferroelectric Bismuth Titanate ($Bi_4Ti_3O_{12}$)'*** submitted by Balram (Roll no. 301104006) in partial fulfillments for the requirements for the awards of Master of Science degree in Physics Department at Thapar University, Patiala is an authentic work carried out by him throughout the year under my supervision and guidance. To the best of my knowledge, the matter embodied in the project has not been submitted to any other University/ Institute for the award of any Degree or Diploma.

Dr. Dwijendra P. Singh

(Assistant Professor),

School of Physics and Materials Science,

Thapar University,
Patiala.

Dr. Kulvir Singh

(Prof. & Head),

School of Physics and Materials Science,

Thapar University,

Patiala.

Dr. S. K. Mohapatra

Dean of Academic Affairs,

Thapar University,

Patiala.

Date: 15-7-2013

Place: Thapar University, Patiala.

Acknowledgements

I express my deep sense of gratitude to my supervisor ***Dr. Dwijendra P. Singh*** (Assistant Professor), School of Physics and Materials Science, Thapar University, Patiala for his valuable guidance and support in carrying out his project. I am also thankful to ***Dr. Kulvir Singh***, Professor and head, School of Physics and Materials Science for providing lab facilities without which this work would not be possible.

I am also very much indebted for valuable suggestion provided by ***Dr. Bhasker Gahtori, Mr. B. Sivaiah*** (Scientists at NPL Delhi).

I owe my heartfelt gratitude to PhD. Scholar ***Ms. Pallavi Gupta, Kriti Tyagi*** for his all-time support and guidance at each and every step of my project work. Without his help it would have been very difficult to complete the work. His deep and clear knowledge in this filed proved to be very fruitful. Thank You Mam for the support and help.

I profusely thank my friend ***Sanjeev Chauhan*** and my dear classmates for their help and support at various steps.

Last but not the least I express my gratefulness to my ***Parents*** without whose blessings and moral support the journey would have become very difficult.

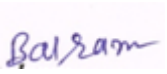

Balram

Roll no. 301104006

Date:15/7/2013

Patiala.

Abstract

The Lead free, Bismuth Titanate (BIT) has been synthesized by Sol-Gel method. The synthesized samples have been subjected to the structural, morphological, hysteresis measurements. The X-Ray Diffraction studies have confirmed that Bismuth Titanate ($Bi_4Ti_3O_{12}$) have the orthorhombic phase without any impurity peak in XRD data. The SEM studies have shown the good surface morphology with varying clusters ranging from 0.5µ to 1µ. The SEM micrograph of BIT indicates that each and every clusters appearing on the surface is comprised of large no. of crystallites. The hysteresis measurement of BIT is also done to confirm the ferroelectric property of the material. The value of P_r and E_c in hysteresis loop is affected by the externally applied field for the drawing the P-E loop. For the higher field, these values are higher as compare to the lower applied electric field (at $12KV/cm^2$, P_r = $0.14451\mu C/cm^2$, E_c = 5.597KV/cm and at $10KV/cm^2$, P_r = $0.12070\mu C/cm^2$, E_c = 4.6456 KV/cm).

Table of Contents

Page no.

List of Figures

List of tables

CHAPTER 1

Introduction

1.1 Motivation and Background

The large scale application of Ferroelectric materials in day to day life in capacitors, sensors, actuators, transducers and memory application demands novel materials of high dielectric constant with low dielectric loss, good piezoelectric as well as pyroelectric properties. Lead-based piezoelectric ceramics with perovskite structure based on lead zirconate titanate (PZT) are widely used for actuators, sensors as well as microelectronic devices because of their excellent piezoelectric properties. However, because of the high toxicity of lead oxide, the use of the lead-based ceramics has caused serious lead pollution and environmental problems devices. The search for novel environmental friendly ferroelectric material is in demand. Among all lead-free piezoelectric materials Bismuth Titanate (BIT), $Bi_4Ti_3O_{12}$ BIT is one of them about which I will go to discuss in this Thesis.

1.2 Bismuth Titanate

Bismuth titanate was discovered by Aurivilius in 1949 [1]. Many of the compositions from the Aurivillius family remain ferroelectric up to significantly higher temperatures than the well known group of ferroelectric perovskite. For example, Bismuth titanate ferroelectric up to 675^0C as compared to ~ 380^0C for lead zirconate titanate. Where the ferroelectric phase allows the alignment of dipole (known as poling) and it is essential for piezoelectricity in ceramics. In which bismuth titanate are phase transition temperature (Curie temperature or T_c) at which Ferroelectricity is lost compared to the high temperature piezoelectric ceramics. It is a ferroelectric material with the chemical formula $Bi_4Ti_3O_{12}$. It has a high Curie-Weiss temperature, ~ 685^0C, high dielectric constant, ~200, and highly anisotropic conductivity [2-5]. Bismuth titanate has recently been receiving attention because of its potential to replace volatile ferroelectrics such as lead containing PZT, as well as for applications in high temperature

environments. Some physical properties of bismuth titanate powders are shown in Table.1 [6].

Table.1: Electrical and Mechanical Properties of $Bi_4Ti_3O_{12}$ Powders [6].

Density ($x10^3 kg/m^3$)	6.55
T_c (^oC)	650
Mechanical Quality Factor Q_M	>600
Maximum Operating Temperature (^oC)	550
Dielectric Constant (1KHz)	120
Planar Coupling k_p	0.03
Longitudinal Coupling k_{33}	0.09
Piezoelectric Coefficient d_{33} ($x10^{-12}$m/V)	18
Piezoelectric Coefficient d_{31} ($x10^{-12}$ m/V)	-2

1.3 Structure of BIT

BIT has a layered perovskite structure represented by the empirical formula ABO_3. The BIT is belongs to the family of ferroelectric materials with layered structures and investigated by Aurivillius in the late 1940s and early 1950s [1]. So that the structure are called Aurivillius phases. The layered structure is constructed by alternative stacking of a triple layer of TiO_6 octahedral (perovskite slab) and a monolayer of $(Bi_2O_2)^{2+}$ along the *c*-axis. Single crystal BIT has a low dielectric permittivity and a very high Curie temperature (T_c = 675^0C).

In fig.1, the two Bi^{3+} ions are located in the A sites of the perovskite block and other two Bi atom are present in the $(Bi_2O_2)^{2+}$ layers. In the bismuth oxide layer Bi-O bonding is likely to covalent [7]. Because the oxygen coordination of Bi in the bismuth oxide layer is less than that of the Bi in the A site of perovskite block. The central octahedral is completely corner shared to the $[TiO_{6/2}]^{2-}$ whereas end octahedral possess one corner in a direction perpendicular to the

layers unshared oxygen. In the $(Bi_2O_2)^{2+}$ layers to the structural entities are $[BiO_{2/2}]^{+}$ which are interconnected and the Bi atoms are severely under coordinated to oxygen's. Thus in BIT it is apparent that there are at least two types of Ti atoms and 5 type of oxygen atoms and two type of Bi atoms which are structurally distinguishable. They are also chemically distinguishable because there are differences in the nature of bonding at these sites [8].

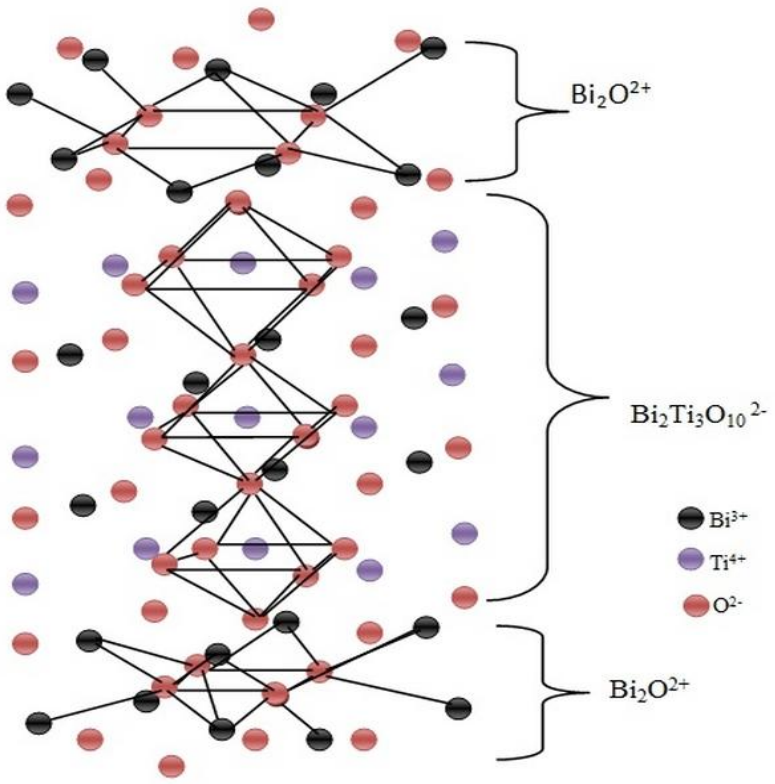

Fig.1: Layered perovskite structure of BIT.

1.4 Application of BIT

Ferroelectric $Bi_4Ti_3O_{12}$ ceramics are potential candidates for device applications due to their high dielectric constant and high breakdown strength [9, 10] Bismuth titanate is most often used in the production of capacitors, transducers, sensors, non-volatile memory, piezoelectric for ultrasound imaging, actuators, electro optic application for data storage application, switches known as transchargers or transpolarizers, oscillators and filters, light deflectors, modulators and displays, etc. as it has a high temperature coefficient of resonant frequency, large dielectric constant and high dielectric losses large leakage current and low remanent

polarization [11]. PTCR properties of Bismuth titanate is most found use as a thermistors e.g. in thermal switches.

1.5 Literature Review

1. Yoleva *et al.,* [12] reported the synthesis of $Bi_4Ti_3O_{12}$ and $Bi_{12}TiO_{20}$ on the basis of hydrolysis-condensation reaction in acetic and nitric medium. By using XRD analysis, IR spectroscopy, SEM and EDS it is finally Conclude that sol gel method is appropriate method for obtaining the phase $Bi_4Ti_3O_{12}$ and $Bi_{12}TiO_{20}$ at lower temperature (600^0C) as compared to other methods.

2. Du *et al*., [13] synthesized Bismuth titanate ($Bi_4Ti_3O_{12}$) by a simple sol-gel method. They indicate that BIT gel decompose in two step posited at approximately 278^0C and 432^0C and BIT began to crystallize before 450^0C. And there is no evidence of formation of an intermediate phase. So after 500^0C they obtained BIT nano-plate like powder and with increase temperature the BIT grain rapidly grew .Then the coalescence of adjacent took place its.

3. Zarycka *et al.,* [14] reports synthesis of randomly oriented $Bi_4Ti_3O_{12}$ (BTO) thin films by a modified hybrid sol-gel process. Crystalline films were deposited on silicon and stainless steel substrates by spin coating and subsequently annealed at 650^0C. The structure of the films was investigated by X-ray diffraction. The formation of a layered perovskite-like structure with orthorhombic symmetry was confirmed. Scanning electron microscopy showed that the surfaces of the films were smooth, dense and crack free. Conservation of the chemical composition was confirmed by energy dispersive spectroscopy.

4. Horn *et al.,* [15] prepared textured bismuth titanate, $Bi_4Ti_3O_{12}$ (BIT) by template grain growth (TGG). They obtained highly textured BIT with the use of only 5 vol% template particles by sintering at 1000^0C for 1 h. The results showed that uniformity of the Through-thickness texture is much higher than reported in the literature for BIT tapes cast with 100% platelets. Initial platelet alignment is shown to increase because of frequent interaction with the fine powder particles during tape casting. By avoiding pressure densification techniques and using only

a small portion of an isometric particle, TGG is a low-cost option for fabricating textured ceramics.

5. Kong *et al.,* [16] synthesized ferroelectric $Bi_4Ti_3O_{12}$ thin films by a hybrid sol gel process. Crack-free and crystalline films of ~ 1mm thickness have been deposited on $Pt/Ti/SiO_2/Si$ substrates. X-Ray diffraction XRD results show that predominant phase of $Bi_4Ti_3O_{12}$ can be obtained at 550^oC, and the films are randomly orientated up to 700^oC. The film annealed at 700^oC, was measured to have a dielectric constant of 105, dielectric loss of 0.04, remnant polarization of 13.5μC/cm^2, and coercive field of 60 kV/cm. The random orientation mechanism and the effect of annealing temperature on the dielectric and ferroelectric properties of the films were qualitatively discussed.

6. Su *et al.,* [17] prepared amorphous bismuth titanate nanoparticles (<50nm) dispersed with poly (hydroxyl ethyl methacrylate) via a sol-gel process. With less than 20% by weight of bismuth titanate in the polymer, the material exhibits high refractive indices (>1.6) and high optical transparency (> 90% transmittance from 530 to 800 nm). Furthermore, the material is highly cross linked has an Improved thermal stability and a lower coefficient of Thermal expansion than that of neat polymer. The material displays a high dielectric constant (>10) without Ferroelectricity. The material has potential applications in optical lenses, optical waveguides and capacitors.

7. Gu *et al.,* [18] synthesized Bismuth titanate powders around the nano meter range using sol-gel process. In this work they give heat treatment, crystallization of the gel into mixture phases from 400°C to 800^oC, formed four phases, at 850^oC, finally transformed to single layered perovskite structure. The particle size of powders increased with calcinations temperature.

8. Shen *et al.,* [19] reported thermal conductivity of c-axis textured polycrystalline perovskite $Bi_4Ti_3O_{12}$ and random polycrystalline material up to 1000°C. Based on measurements of the thermal diffusivity, density and specific heat, the thermal conductivity is lower along the c-axis than in the a-b plane by almost a factor of 2, and the anisotropy persists up to at least 1000°C despite a

change in the crystal structure at 675 °C. The exceptionally low (1.0W/mK), temperature-independent conductivity perpendicular to the perovskite layer structure is attributed to the density difference between the pseudo perovskite and fluorite blocks in the unit cell, forming a natural nano structured superlattice.

9. Slavov *et al.,* [20] synthesized Bismuth-titanate ceramics doped with SiO_2 and Nd_2O_3 by melt quenching method in the system of Bi_2O_3-TiO_2-Nd_2O_3-SiO_2 with temperature range of 1250–1500°C. Different values of conductivity, dielectric losses and relative permittivity are obtained which depend upon the composition. Finally they observed that all investigated samples are dielectric materials with conductivity between 10^{-9} and 10^{-13} $(\Omega \cdot cm)^{-1}$ at room temperature, dielectric permittivity from 1000 to 3000 and dielectric losses tan δ between 0.0002 and 0.1.

10. Cheng *et al.,* [21] reported the thin film of calcium doped ferroelectric bismuth titanate $CaBi_4Ti_4O_{15}$ (CBT) by sol-gel method and film deposited on ITO/glass substrates. The ferroelectric properties in annealed CBT thin films showed and exhibited clear polarization versus electrical field curves. From P-E curves, the $2P_r$ value and coercive field of annealed CBT thin films were calculated to be 10μC/cm^2 and 180kV/cm, respectively.

11. A very nice study has been carried out by Lazarevic and their group [22]. They prepared ferroelectric bismuth titanate by using different method, depending if the creation will be film coating or ceramics. They observed the structural properties and various other properties of Bismuth titanate which show a significance dependence on the applied synthesis method.

Chapter 2

Characterization Techniques

Success in devising and collecting systems on the scale of nanometers require a deeper Understanding of the basic processes and phenomena involved. Hence, one of the current key objectives is to adapt and develop a range of techniques that can characterize the structural, thermal, electronic, magnetic, dielectric, composition, electrical and optical properties of the nanostructure systems. These techniques include X-Ray Diffraction, Scanning Electron Microscope (SEM), and P-E Loop measurements. In this chapter, the synthesis and characterizations for preparation of BIT $Bi_4Ti_3O_{12}$ ferroelectric ceramics are discussed in details:

2.1 X-Ray Diffraction (XRD)

In X-ray diffraction or scattering (XRD), X-ray photons are utilized to probe the matter. The energy of the emitted radiation is specific for each element. X-rays were discovered by Roentgen, he called them X-rays because their nature at first was unknown so, X-rays were also called Roentgen rays. The X-rays lie in the range of $0.1\ Å < \lambda < 1000\ Å$. The penetrating power of X-rays depends on energy.

2.1.1 Principle

X-Ray diffraction effects are observed when electromagnetic radiation impinges on periodic structures with geometrical variations comparable to the length scale of the wavelength of the radiation. X-ray diffraction is based on constructive interference of monochromatic X-rays and a crystalline sample. These X-rays are generated by a cathode ray tube, filtered to produce monochromatic radiation, collimated to concentrate and directed towards the sample. X-rays are generated when high velocity electrons impinge on a metal target. Approximately 1% of the total energy of the electron beam is converted into X-ray radiation. In order to get a narrow beam of X-rays, the X-rays generated by the target material are allowed to pass through a collimator which consists of two sets of closely packed metal plates separated by a small gap. The collimator absorbs all the X-rays except the narrow beam that passes between the gaps [23, 24].

2.1.2 Bragg's Law

Diffraction is a scattering phenomenon. When X-rays are incident on crystalline solids then they are scattered in all directions. In some of these directions the scattered beams are completely in phase and reinforce one another to form the diffracted beams as shown in fig.2. The Bragg law describes the conditions under which this would occur. It is assumed that a perfectly parallel and monochromatic X-ray beam of wavelength λ is incident on a crystalline sample at an angle θ [25].

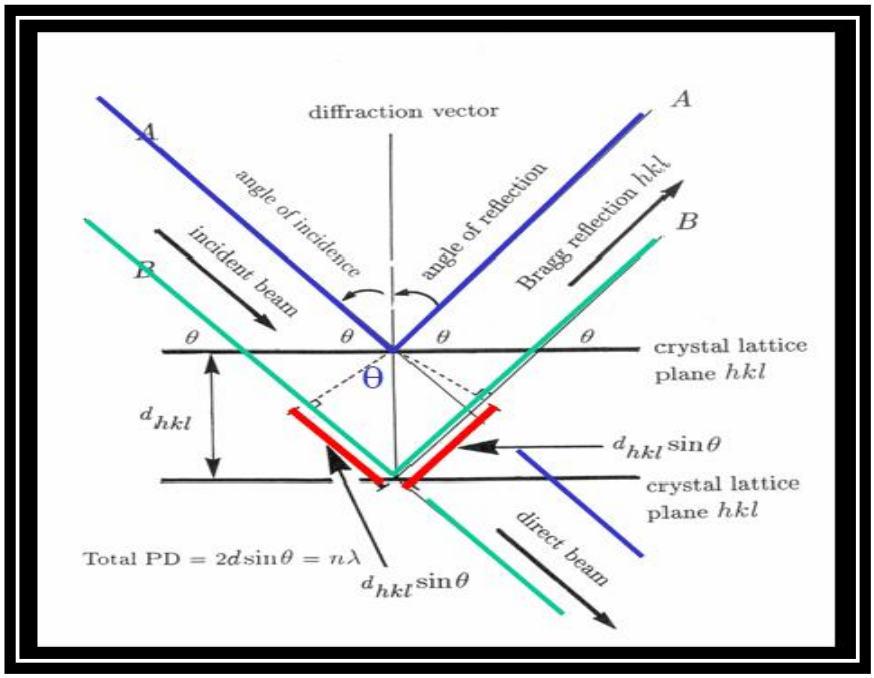

Fig.2: X-ray diffraction for Bragg's law.

The General relationship between the incident ray of wavelength, incident angle and spacing between two rays are diffracted or crystal lattice planes of particle or atoms is known Bragg's law and given relation in Eq. (1)

$$n\lambda = 2d\text{Sin}\theta \ldots\ldots\ldots\ldots\ldots\ldots\ldots\ldots\ldots\ldots (1)$$

Where d is the spacing between atomic planes in the crystalline phase and λ is the X-ray wave length. The intensity of the diffracted X-rays is measured as a function of the diffraction angle 2θ and the specimen's orientation.

2.1.3 Experimental Setup

Fig.3: XRD apparatus.

2.2 Scanning Electron Microscope (SEM)

The scanning electron microscopy (SEM) is a useful technique to study the topography and morphology of the materials with much higher resolution. The working principle of SEM is that when a beam of highly energetic electrons strikes the sample, the secondary electrons, x-rays and back-scattered electrons are ejected from the sample as shown in fig.4. These electrons are then collected by the detector and convert into signal that displays on a screen. This wide spread use of electron microscopes is based on the fact that they permit the observation and characterization of materials on a nanometer (nm) to micrometer (μm) scale. It is widely used by the researchers in order to get

- Topography: Information about the surface of the object.
- Morphology: The size and shape of the particles making the object.

In the present study, the SEM micrograph was taken on the fractured surface of the sample using scanning electron microscope (SEM: JSM-840 scanning microscope JEOL as shown in fig.5). The samples were made conducting by coating a thin layer of platinum using a sputter coater. For the measurement of grain size, lines of known length were drawn on the micrograph. The number of

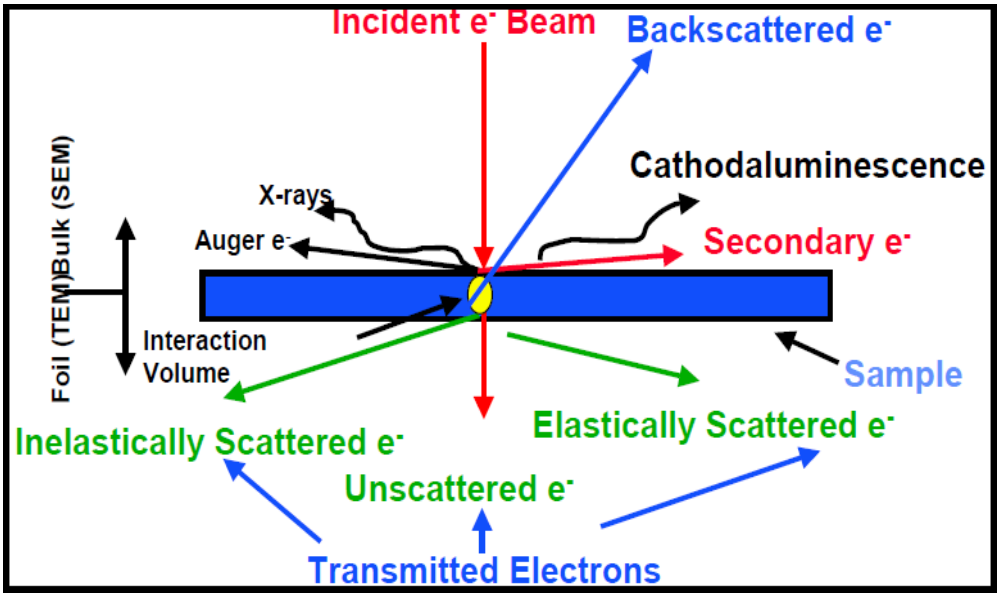

Fig.4: Principle of Scanning Electron Microscope (SEM).

Grain size, lines of known length were drawn on the micrograph. The number of grains that were cut by the lines was counted. The average grain sizes were then calculated by dividing the length of the line by the number of grains coming under that line. A minimum of 10 lines, each of length not less than 200 micrometers were drawn on the different places of a single micrograph and average grain sizes were calculated to minimize the error.

2.3 Hysteresis Measurement

The polarization versus electric field (P-E) hysteresis loop is one of the most important electrical characteristic of ferroelectric ceramics. Hysteresis loop comes to the various sizes and shapes and which can be used to identify the materials. Hysteresis loops can be information for the understanding of ferroelectric materials. For example the materials with a square-like P-E loop as shown in fig.6 have memory ability. A high remanent polarization is related to the high internal

Fig.5: Apparatus of Scanning Electron microscope (SEM: JSM-840 scanning microscope JEOL).

Polarizability, strain, electromechanical coupling, and electro optic activity. For a given material, the coercive field (E_c) is an indication of the grain size of material (i.e., lower E_c means larger grain size and higher E_c means smaller grain size). A high degree of loop squareness usually indicates better homogeneity and uniformity of grain size of materials. For relaxor ferroelectric materials, the high

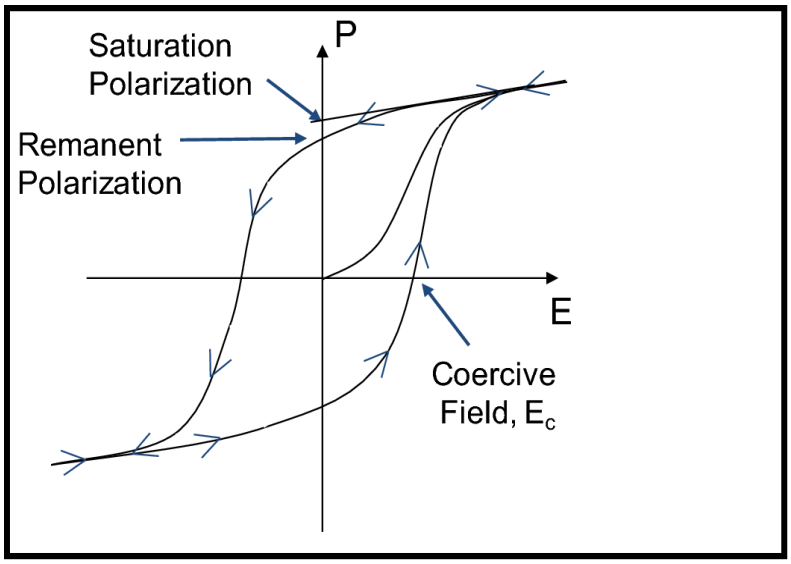

Fig.6: Hysteresis loop of ferroelectric material (P-E Hysteresis).

Induced polarization means high electrostriction strain and high electro optic coefficients. A sudden large change in apparent polarization is usually an indication of incipient dielectric breakdown [26]. The ferroelectric hysteresis loop depends on the temperature that mean the temperature increases the loop of width and height will be changing. At the particular temperature behaves of the materials visible and loops are merging to the straight line. This particular temperature called Curie temperature of ferroelectric materials [27].

2.4 Synthesis

Ferroelectric materials are found mainly in three form Nano, Bulk and thin film. There are different methods for the fabrication of these three different forms of ferroelectric materials as shown in Table. 2

Table.2: Different methods for fabrication of ferroelectric materials:

Methods to diff. form of material	**Different Routes**
Nano	Sol Gel route [17], hydrothermal synthesis [28], solvothermal method [29] etc.
Bulk	Solid state route [30], Sol Gel method etc.
Thin film	Sol-Gel, Chemical Solution Deposition(CSD) [31], Sputtering [32], Pulsed Laser deposition [33] and Metal Organic Chemical Vapour Deposition (MOCVD) [34] etc.

Out of these, sol-gel method has many advantages over other methods and was chosen for the fabrication of Bismuth Titanate**.** Therefore we choose it for our dissertation.

2.4.1 Sol gel synthesis

The sol-gel process is a wet chemical technique widely used in the field of material science and ceramic engineering. Such methods are used primarily for the fabrication of materials (typically a metal oxide). The sol-gel process, as the

name implies, involves the evolution of inorganic networks through the formation of a colloidal suspension (sol) and gelation of the sol to form a network in a continuous liquid phase (gel). The starting material is processed to form a dispersible oxide and forms a sol in contact with water or dilute acid. During the process, the sol yields the gel, and the sol/gel transition controls the particle size and shape. Sol-gel processing refers to the hydrolysis and condensation of alkoxide-based precursors. The reactions involved in the sol-gel chemistry is based on the hydrolysis and condensation of metal alkoxide M (OR), it can be described as follows:

$$MOR + H_2O \rightarrow MOH + ROH \text{ (hydrolysis)}$$

$$MOH + ROM \rightarrow M\text{-}O\text{-}M + ROH \text{ (condensation)}$$

The sol-gel process can be characterized by a series of distinct steps:

- The first step consists of the formation of different stable solutions of the alkoxide or solvated metal precursor (the sol).
- In the second step, gelation begins, which results in the formation of an oxide- or alcohol-bridged network (the gel) by a poly-condensation or poly-esterification reaction that results in a dramatic increase in the viscosity of the solution.
- The third step is the aging of the gel, during which the poly-condensation reactions continue until the gel transforms into a solid mass, accompanied by contraction of the gel network and expulsion of solvent from gel pores. It is referred to as coarsening, phenomenon by which smaller particles are consumed by larger particles during the growth process and phase transformations may occur concurrently with synthesis.
- The fourth step is drying of the gel, when water and other volatile liquids are removed from the gel network. This process is complicated due to fundamental changes in the structure of the gel. The drying process has itself been broken into four distinct steps: (i) the constant rate period, (ii) the critical point, (iii) the falling rate period, (iv) the second falling rate period. If isolated by thermal evaporation, the resulting monolith is termed a xerogel. If the solvent (such as water) is

extracted under supercritical or near super critical conditions, the product is an aerogel.

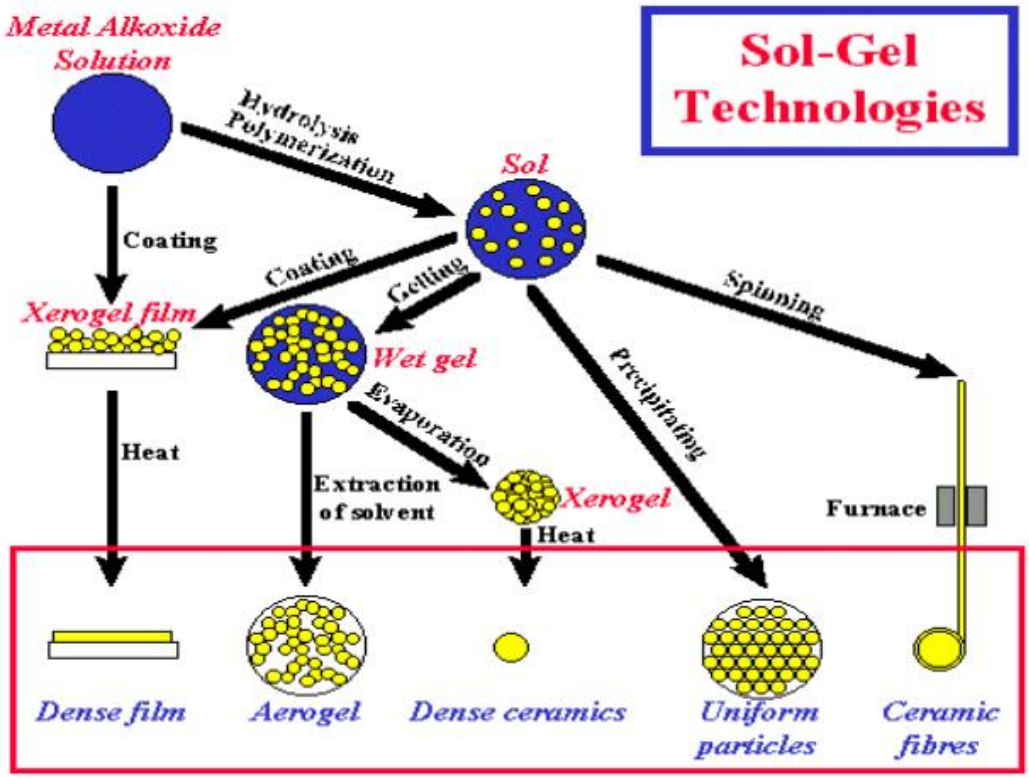

Fig.7: Schematic representation of Sol-Gel process for synthesis of Nanoparticles.

- The fifth step involves dehydration, during which surface-bound M-OH groups are removed, thereby stabilizing the gel against rehydration.
- Thermal treatment: calcinations and sintering.

2.4.2 Sol-Gel Chemistry

The selection of precursors (i.e. starting compound) is very important in sol-gel process. The ideal compound to be used as precursor should satisfy the following criteria:

- It should have high metal content: To minimize the volume change during the change from metal-organic solution to inorganic powder.
- High solubility in common solution with other starting compounds. It should be chemically compatible with other compounds.

- Cost effective to produce: as the capital equipment requirements are small (e.g. no high vacuum systems are needed), so the cost of sol-gel process is low, and precursor should not change this advantage.
- Thermally decompose without evaporating, melting or leaving carbon content.

2.4.3 Selection of solution

- Solutions have high vaporization rates: they should evaporate as early as possible. Vaporization depends on vapour pressure and interaction between solute and solvent.
- Solvent must be carefully being selected in order to get solution of high concentration of necessary components, proper viscosity and proper surface tension.

2.4.4 Advantage of sol-gel processing

- **Versatile**: better control of structure, including porosity and particle size possibility of incorporating nanoparticles and organic materials into sol-gel matrix.
- **Extended composition ranges**: allows the fabrication of any oxide composition but also some non-oxides and hybrid organic-inorganic materials.
- **High homogeneity**: due to mixing at the molecular level (chemical nanotechnology) high purity.
- **Less energy consumption**: no need to reach the melting temperature since a dense of network structure can be achieved at lower temperatures near T_c.
- **Any shape:** thin films and coatings, monoliths, composites, porous membranes and powders and fibers.
- **Cheap:** no need for special or expensive equipment. It provide a simple, economic and effective method to produce high Quality coatings.

2.5 Calcination

The well grinded powders were taken in an alumina crucible for calcinations in POT furnace at particular temperatures according to sample. It is a thermal treatment process applied to ores and other materials in ores and other materials in order to bring about a thermal decomposition phase transition or removal of a volatile fraction.

1. It is a heat treatment process which promotes diffusion.
2. Temperature of calcination must be less than the temperature of melting of the materials, which differs from materials to materials.

$$\mathbf{T_{calcination} < T_{melting\ point}}$$

At $\mathbf{T_{calcination}}$ Gibb's free energy is Zero. It influences density and electromechanical property of final product, inter diffusion of ions of the constituents, and phase transition. Greater $\mathbf{T_{cal}}$ suggests greater homogeneity of the final product, as it can be heated to a greater extent.

2.6 Sintering

Density of the electronic ceramic is a very sensitive parameter and that directly affects their properties. Therefore, proper sintering of the pellets is essential for electrical measurement. The pellets were taken on an alumina plate and sintered at different temperatures in POT furnace at a heating rate of 5^{o}C per minute at 750^{0}C, for volatile fraction removal if any in the initial heat treatment.

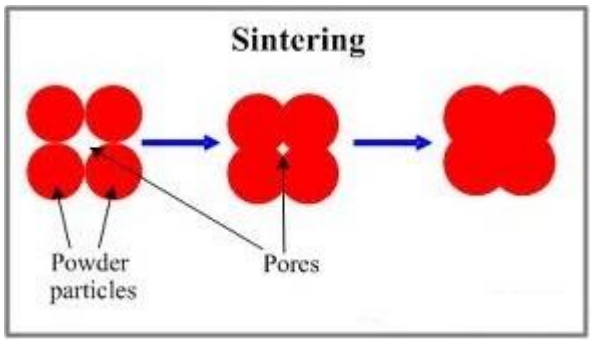

Fig. 8: Densification process.

It is the process of consolidation of either loose aggregate of powder or a green compact of the desired composition under controlled conditions of temperature and time.

Densification occurs during sintering and solid state sintering is carried out at temperatures where material transport due to diffusion is appreciable. Atomic diffusion is required, since surface diffusion is required. In between the granules, a small granule is present, when pressured the surface area increases and the material gets densified. Densification process is shown in fig 8.

2.7 Preparation of sample

First solution is prepared by using Bismuth nitrate (≥99%, Shanghai Chemical Industry, Shanghai, China) dissolved in Acetic acid (Sigma Aldrich, 99%) at room temperature with an equilibrium molar ratio Acetic acid: Bismuth nitrate for 30:1. The solution taken constant stirred by magnetic stirring at 40 ^{0}C for 30 min. In the heating solutions are adding the deionized water at ratio H_2O: Bi $(NO_3)_3$.$5H_2O$ for 6:1. Second solution take Titanate (iv) Isoproxide (Sigma Aldrich 97%) in the 2- methoxyethanol (Sigma Aldrich, 97%) at room temperature with molar ratio Titanate (iv) Isoproxide : 2- methoxyethanol for 30 : 1 and taken at stirred by magnetic stirring at 40 ^{0}C for 30 min. After the above process both solution first and second mixed at room temperature and continues stirred for 30 min until we get a transparent solution. To increase the solution stability adds 10 ml Acetyl acetone (Sigma Aldrich, 99%). After adding acetyl acetone the color of the solution gets changed. This solution was remained as it is for 18 hours at room temperature. After that it was heated at 40 ^{o}C on magnetic stirrer along with slow stirring until we got the powder form. Then grind the powder form we get with help of Mortar Pestle. Then it was Calcined at 500 ^{0}C for 14 hours. Then again grind the Calcined powder for around 10 minutes with Mortar Pestle. Then pellets were made with help of die punch machine. These pellets were sintered at 750^{o}C. Then the various measurements were done.

2.8 Experimental flow chart

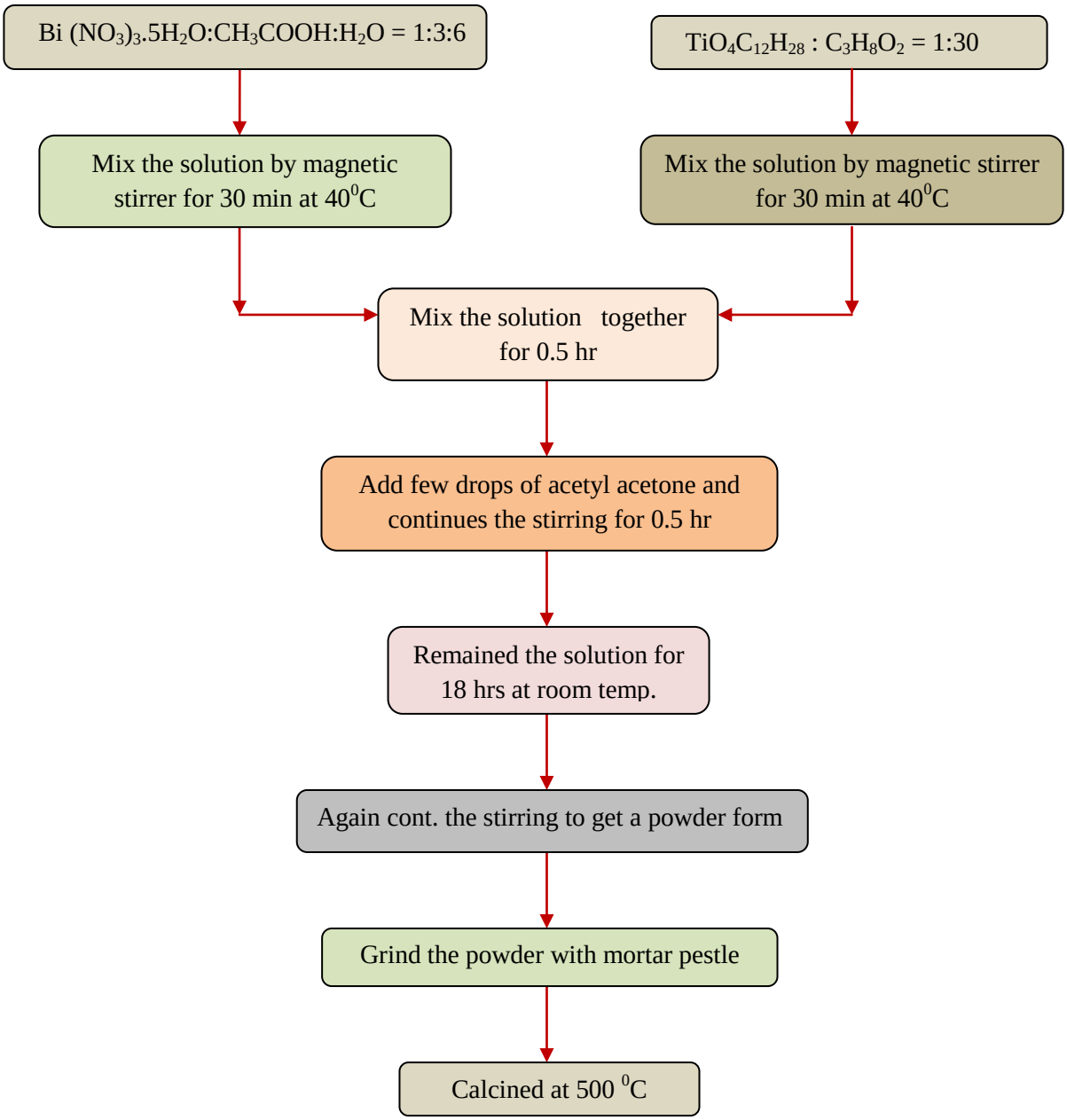

Fig.9: Flow chart for the preparation of BIT by sol-gel method.

Chapter 3

Results and Discussion

The structural, morphological and ferroelectric properties are carried out by using XRD, SEM and P-E loop respectively. The Results of these experimental investigations are discussed in the subsequent subsection.

3.1 XRD Analysis

Calcined powder of Bismuth titanate was subjected to phase analysis by X-ray diffraction. This is done to know the different phases present in the Calcined powder. The angle range was 20^{o}-70^{o}. Fig.10 shows the XRD diffractogram of $Bi_4Ti_3O_{12}$ nanoparticles, where all the major peaks are indexed and well-matched to the orthorhombic structure with cell parameters a = c = 5.4489A^{o}, b= 32.8156A^{o} (File name xrd2288). The crystallite size of synthesized nanoparticles was calculated by Scherrer's formula, as given below:-

$$d = \frac{k\lambda}{\beta Cos\theta}$$

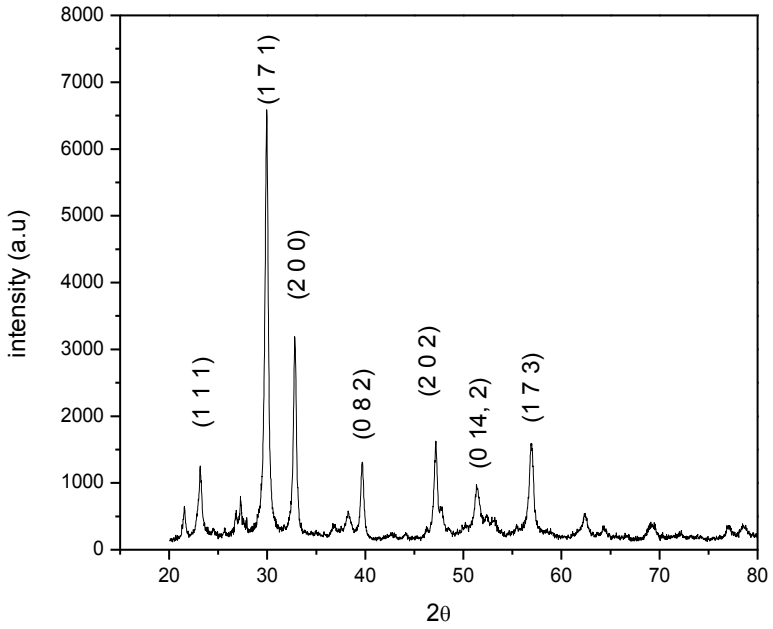

Fig.10: XRD pattern of Bismuth Titanate ceramics.

where k is the shape factor (k = 0.94), λ is the x-ray wavelength, β is the line broadening at half the maximum intensity (FWHM) in radians, and θ is the Bragg's angle, d is the crystallite size. The crystallite size for $Bi_4Ti_3O_{12}$ nanoparticles was found to be ~19 nm. The XRD pattern shows that the sample contains no impurity peak and match with JCPDS card number 00-035-0795. The pattern in the fig. 9 shows the clear single orthorhombic phase without any secondary phase.

3.2 SEM analysis:

SEM micrograph of Calcined powder of Bismuth Titanate with different magnification is shown in the fig.11. Sample shows good surface morphology with varying clusters ranging from 0.5μ to 1μ. Actually these are not representing

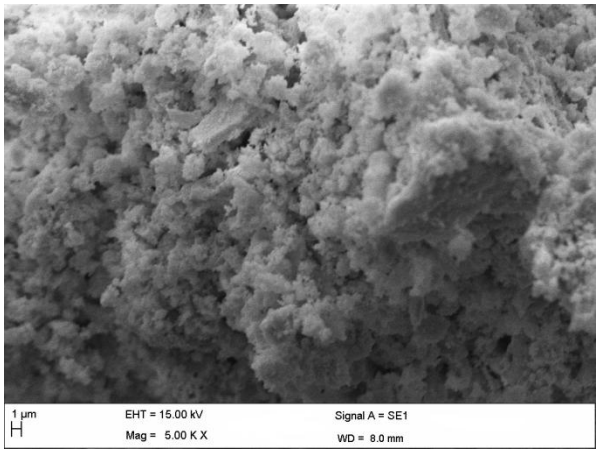

(a)

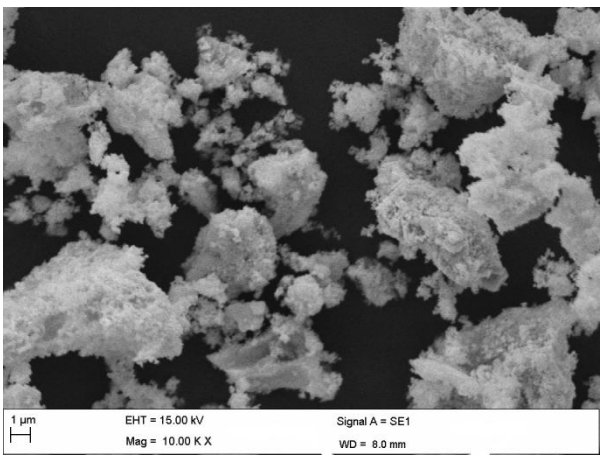

(b)

Fig.11: SEM micrograph of BIT with different magnification.

the grain size because the grain size evaluated by Scherrer's formula is coming out to be ~19 nm, and here the values are much larger than the grain size. Therefore, SEM micrograph indicates that each and every clusters appearing on the surface is comprised of large no. of crystallites.

3.3 P-E loop measurement

The hysteresis measurement is done to confirm the ferroelectric property of the material. A P-E loop tracer shows a plot of the polarization (P) versus applied ac field to (E) at a given frequency. The spontaneous polarization (P_s), remnant polarization (P_r) and the coercive field (E_c) can be measured by studying the hysteresis loop. Fig.12 shows the polarization vs. electric field curves for samples sintered at 750 ^oC. It can be seen that the value P_r and E_c is affected by the

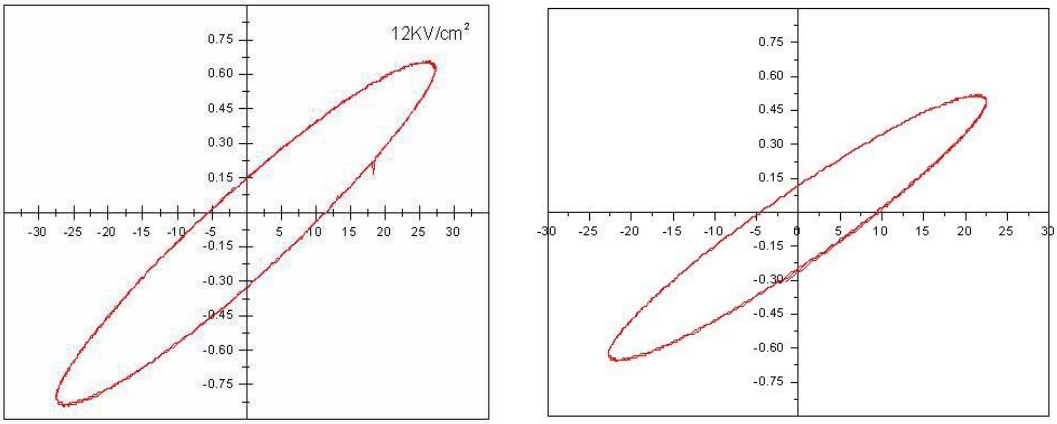

(a) (b)

Fig.12: Hysteresis loop measurement of BIT.

externally applied field for the drawing the P-E loop. For the higher field, these values are higher as compare to the lower applied electric field (at 12KV/cm^2, P_r = 0.14451μC/cm^2, E_c = 5.597KV/cm and at 10KV/cm^2, P_r = 0.12070μC/cm^2, E_c = 4.6456 KV/cm) When the field is high then the dipole formed between the titanium and oxygen ion is aligning in a better way as compared to lower field. In this way, the applied electric field is serving the purpose of pre-polling.

CHAPTER 4

Conclusions and Future Scope

The conclusions of characterization and synthesis are follows:

4.1 Conclusions

The discussed results in earlier chapter can be concluded as follows

1. The sample has been successfully synthesized by sol gel method.
2. The XRD studies has confined the BIT crystallizes into single orthorhombic phase with lattice parameter a = c = 5.4489A^o, b= 32.8156A^o.
3. The crystalline size is calculated by using Debye Scherrer's formula and it is found to be ~19 nm.
4. The SEM studies are showing the good morphology, but not properly sealed grains. But it is representing the cluster; which is the combination of large number of crystallites.
5. The ferroelectric behavior of BIT is confined by studying the P-E loop. Since, the electric polling of the sample was not done; therefore it is showing the applied electric field dependent E_c and P_r. Therefore the value of E_c and P_r at high field is found to be 5.597KV/cm, 0.14451μC/cm^2 resp.

4.2 Future Scope

The studies present in this thesis are very preliminary in nature. Therefore, some valuable and applicable investigation of BIT is required. The following are the suggestion for the future scope of studies:

1. The capacitive behavior of BIT should be investigated in detail by making M-I-M capacitor.
2. The composite of BIT with polymer can be used for applying it in modern electronics.
3. The relaxation of dipoles with electric field and temperature is very important. That also needs to be investigated.

Reference

[1] Aurivilius. B, *Arkiv Kemi,* 1(1949).

[2] Lazarevic, Z., Stojanovic, B.D., Varela, J.A, *Science of Sintering.* 37, 199 (2005)

[3] Smolenskii, G. A., Bokov, V. A., Isupov, V. A., Kranik, N. N., Pasynkov, R. E., Sokolov A.I.(1984). *Ferroelectrics and Related Materials*. New York, NY: Gordon and Breach Science Publishers.

[4] Cummins, E. Cross, L.E, *J. Appl. Phys.* 39(5) 1968.

[5] Dorrian, J. F., Wolfe, R.W., Newnham, R. E., *Ferroelectr.* 3, 17 (1971).

[6] Kobayashi, M. Jen, C.-K., Ono, Y., Kruger, S., *IEEE Ultrasonic's Symposium,* 910 (2004).

[7] S. Ezhilvalavan, J. M. Xue, John Wang, Mater. *Chem. Phys.* 75, 50 (2002).

[8] M. Lines, A. Glass, Clarendon Press, Oxford, 87 (1977).

[9] J. F. Dorrian, R. E. Newnham, K. K. Smith, *Ferroelectrics*, 3, 17 (1971).

[10] H. S. Shulman, M. Testorf, D. Damjanovic, N. Setter, *J. Am. Soc.*, 79, 3214 (1996).

[11] J. Valasek, *Phys. Rev.*, 17, 475 (1921).

[12] A.Yoleva, S. Djambazov, Y. Ivanova, E. Kashchieva., *Journal of the University of Chemical Technology and Metallurgy*, 46, 255 (2011).

[13] Xianfeng Du, Youlong Xu, Hanxiao Ma, Jie Wang, and Xifei Li, *J. Am. Ceram. Soc.*, 91, 2079 (2008).

[14] Aldona Zarycka, Agata Lisińska-Czekaj, Justyna Czuber, Tomasz Orkisz, Jan Ilczuk, Dionizy Czekaj, *Mater. Sci. -Poland*, 23, (1), (2005).

[15] Jeffrey A. Horn, S. C. Zhang, U. Selvaraj, Gary L. Messing, and Susan Trolier-McKinstry, *J. Am. Ceram. Soc.*, 82, 921 (1999).

[16] L.B. Kong, J. Ma, *Thin Solid Films*, 379, 89 (2000).

[17] Wei-Fang Su Jiann-Fong Lee Ming-Yao Chen Bulletin of the College of Engineering, N.T.U.,89, 29 (2003).

[18] Haoshuang Gu, Peizhi Chen, Youhua Zhou, Min Zhao, Anxiang Kuang, and Xingjiao Li, *Ferroelectr.*, 211, 271 (1998).

[19] Yang Shen, David R. Clarke, and Paul A. Fuierer, *Appl. Phys. Lett.* 93, 102907 (2008).

[20] Stanislav S. Slavov, Milena Z. Krapchanska, Elena P. Kashchieva, Svetlin B. Parvanov, Yanko B. Dimitriev, *Processing and Application of Ceramics* 6, 117 (2012).

[21] Chien-Min Cheng, Ming-Chang Kuan, Kai-Hunag Chen, Jen-Hwan Tsai, *Int. J. Mod. Phys.*, 6, 91 (2012).
[22] Z. Lazarević, B. D. Stojanović, J. A. Varela, *Science of Sintering*, 37(2005) 199.
[23] B. K Tanner *et al.*, *Appl. Surf. Sci.*, 182, 202 (2001).
[24] Warren, X-ray Diffraction, Addison-Weslay, reading, M A, (1969).
[25] V. Raghwan, *Mater. Sci. Eng.*. PHI Learing (2004).
[26] L. B. Kong, T. S. Zhang, J. Ma and Y. C. F. Boy, *Thin solid films*, 379, 89 (2000).
[27] I. Mayergoyz and G. Bertotti, *The science of hysteresis*, volume 3 (Eds.); Elsevier (2005).
[28] Haoshuang Gu, Zhenglong Hu, Yongming Hu, Ying Yuan, Jin You, Weidong Zou, *Colloids Surf. A*, 315, 294 (2008).
[29] Richard I. Walton, *Chem. Soc. Rev.*, 31, 230 (2002).
[30] Wei Li, Kai Chen, Yangyang Yao, Jinsong Zhu, and Yening Wang, *Appl. Phys. Lett.*, 85, 4717 (2004).
[31] Hiroshi Uchida, Isao Okada, Hirofumi Matsuda, Takashi Iijima, Takayuki Watanabe, and Hiroshi Funakubo, *Integr. Ferroelectr.*, 52, 41 (2003).
[32] P. K. Ghosh, A. S. Bhalla, and L. E. Cross, *J. Mater. Sci.*, 29, 4659 (1994).
[33] R. Ramesh, K. Luther, B. Wilkens, D. L. Hart, E. Wang, J. M. Tarascon, A. Inam, X. D. Wu, and T. Venkatesan, *Appl. Phys. Lett.*, 57, 1505 (1990).
[34] L. W. Fu, H. Wang, S. X. Shang, X. L. Wang, and P. M. Xu, J. Cryst. Growth, 139, 319 (1984).